JOURNAL OF QUATERNARY SCIENCE (2010) **25**(7) 1063–1075

Published online in Wiley Online Library
(wileyonlinelibrary.com) DOI: 10.1002/jqs.1263

Holocene climatic fluctuations and positioning of the Southern Hemisphere westerlies in Tierra del Fuego (54° S), Patagonia

NICOLAS WALDMANN,[1*†] DANIEL ARIZTEGUI,[1] FLAVIO S. ANSELMETTI,[2] JAMES A. AUSTIN JR,[3] CHRISTOPHER M. MOY,[4] CHARLES STERN,[5] CRISTINA RECASENS[1] and ROBERT B. DUNBAR[4]

[1] Section of Earth and Environmental Sciences, University of Geneva, Geneva, Switzerland
[2] Eawag (Swiss Federal Institute of Aquatic Science & Technology), Department of Surface Waters, Duebendorf, Switzerland
[3] Institute for Geophysics, John A. and Katherine G. Jackson School of Geosciences, University of Texas at Austin, Austin, Texas, USA
[4] Department of Geological and Environmental Sciences, Stanford University, California, USA
[5] Department of Geological Sciences, University of Colorado at Boulder, Boulder, Colorado, USA

Waldmann, N., Ariztegui, D., Anselmetti, F. S., Austin, Jr J. A., Moy, C. M., Stern, C., Recasens, C., Dunbar, R. B. 2010. Holocene climatic fluctuations and positioning of the Southern Hemisphere westerlies in Tierra del Fuego (54° S), Patagonia. *J. Quaternary Sci.*, **Vol. 25** pp. 1063–1075. ISSN 0267-8179.

Received 15 July 2008; Revised 27 November 2008; Accepted 22 December 2008

ABSTRACT: Recent advances in the chronology and the palaeoclimatic understanding of Antarctic ice core records point towards a larger heterogeneity of latitudinal climate fluctuations than previously thought. Thus, realistic palaeoclimate reconstructions rely in the development of a tight array of well-constrained records with a dense latitudinal coverage. Climatic records from southernmost South America are critical cornerstones to link these Antarctic palaeoclimatic archives with their South American counterparts. At 54° S on the Island of Tierra del Fuego, Lago Fagnano is located in one of the most substantially and extensively glaciated regions of southernmost South America during the Late Pleistocene. This elongated lake is the largest (~110 km long) and non-ice covered lake at high southern latitudes. A multi-proxy study of selected cores allows the characterisation of a Holocene sedimentary record. Detailed petrophysical, sedimentological and geochemical studies of a complete lacustrine laminated sequence reveal variations in major and trace elements, as well as organic content, suggesting high variability in environmental conditions. Comparison of these results with other regional records allows the identification of major known late Holocene climatic intervals and the proposal for a time for the onset of the Southern Westerlies in Tierra del Fuego. These results improve our understanding of the forcing mechanisms behind climate change in southernmost Patagonia. Copyright © 2009 John Wiley & Sons, Ltd.

KEYWORDS: high-latitude palaeoclimate; orbital forcing; lacustrine basins; mid Holocene optimum; Little Ice Age; tephrochronology.

Introduction

The Southern Hemisphere westerlies have a considerable influence on the Southern Ocean circulation and therefore on global climate (Toggweiler and Samuels, 1995; Rahmstorf and England, 1997; Klinger *et al.*, 2003; Garreaud *et al.*, 2009). General circulation models suggest that intensity and latitudinal position of the westerlies have changed since the Last Glacial Maximum (LGM) (Kutzbach *et al.*, 1993; Wyrwoll *et al.*, 2000); however, there are very few high-resolution palaeoclimate proxy records from southern South America that can adequately test these findings. In addition, many of these records that do exist are not necessarily in agreement (Heusser, 1989; Haberzettl *et al.*, 2005; Kilian *et al.*, 2007). The permanent flow of cold polar air from Antarctica causes a strong meridional air temperature gradient in the southern mid latitudes (Thompson and Wallace, 2000). The Island of Tierra del Fuego, at the southernmost extreme of South America, is directly situated in the path of the Southern Westerlies during austral summer.

Here we present a continuous and high-resolution continental sedimentary archive from Lago Fagnano in Tierra del Fuego. Sediment cores obtained from this large lake provide evidence for rapid fluctuations in climate related to changes in the strength and latitudinal position of the Southern Westerlies belt during the Holocene. Our main goal for this paper is therefore to characterise Holocene sedimentation using physical and chemical properties. In this and forthcoming publications, we will use the palaeoclimate records derived

* Correspondence to: N. Waldmann, Department of Earth Science, University of Bergen, Allegaten 41, 5007 Bergen, Norway.
E-mail: nicolas.waldmann@geo.uib.no

from this lake in order to address several long-standing issues related to the timing and phase of climate variations in the Southern Hemisphere. Further comparisons to other marine and continental archives in southern South America and Antarctica will improve our understanding of the forcing mechanisms behind climate change and validate the outcome of existing ocean and atmospheric climatic models for the Southern Hemisphere.

Study area

The island of Tierra del Fuego is the world's southernmost large landmass with the exception of Antarctica. The island is bounded by the southern Atlantic Ocean to the east and the southern Pacific Ocean to the west (Fig. 1). At ~54° S, Lago Fagnano (or Lago Kami in the native Yamana language) lies at the southern part of the island in one of the most important and extensive Late Pleistocene glaciated regions of South America. With a total area of about 560 km^2, this oligotrophic (Mariazzi *et al.*, 1987), latitudinally elongated lake of ~105 km length with a maximal width of ~10 km is the southernmost and largest ice-free lake in the world.

The origin and development of Lago Fagnano are due to a combination of climatic and tectonic processes. The lake is located along a major plate boundary separating the Scotia and South American plates, and during past glacial periods ice originating from the Cordillera Darwin has expanded eastwards through the Fagnano basin and terminated east of the modern lake margin. Glacial sediment accumulation probably covers the entire Holocene and may date back even to the LGM (Bujalesky *et al.*, 1997). Currently, the climate of this region is alpine, with a strong winter subpolar Antarctic influence and under the south-westerly wind effect during austral summers, which brings moisture and humidity to the region. This situation, however, may have changed since the Lateglacial period, as is recorded by other southern Patagonian archives (e.g. Douglass *et al.*, 2005; Gilli *et al.*, 2005; Moy *et al.*, 2008).

The lake comprises two sub-basins: a smaller, deeper basin in the east reaching a maximum depth of 200 m, and an elongated, shallower basin in the west with a maximum water depth of ~120 m (Fig. 1(D)). The southern shores are bordered by the foothills of Sierras de Alvear (eastern extension of the Cordillera Darwin), while the lower elevation mountain belt of the Sierras de Beauvoir borders the northern margin of the lake. The Claro, Milna, Valdez and Turbio rivers discharge into this lake, whereas the Azopardo River at the western extreme of the lake is the only outlet towards the Pacific Ocean through the Seno Almirantazgo (Admiralty Sound) and the Straits of Magellan (Fig. 1(C)).

The lake occupies the deepest continental pull-apart basin in a series of asymmetric tectonic grabens organised in an *en-échelon* arrangement along the Magellan–Fagnano Transform (MFT) (Lodolo *et al.*, 2003, 2007; Menichetti *et al.*, 2008; Tassone *et al.*, 2008). The onset of horizontal left-lateral movement along the MFT is not well dated, but is presumed to have started during the Oligocene (Klepeis, 1994; Lodolo *et al.*, 2003). Recent fault scarps and displacement of glaciolacustrine sediments along the transform lineation in the eastern part of

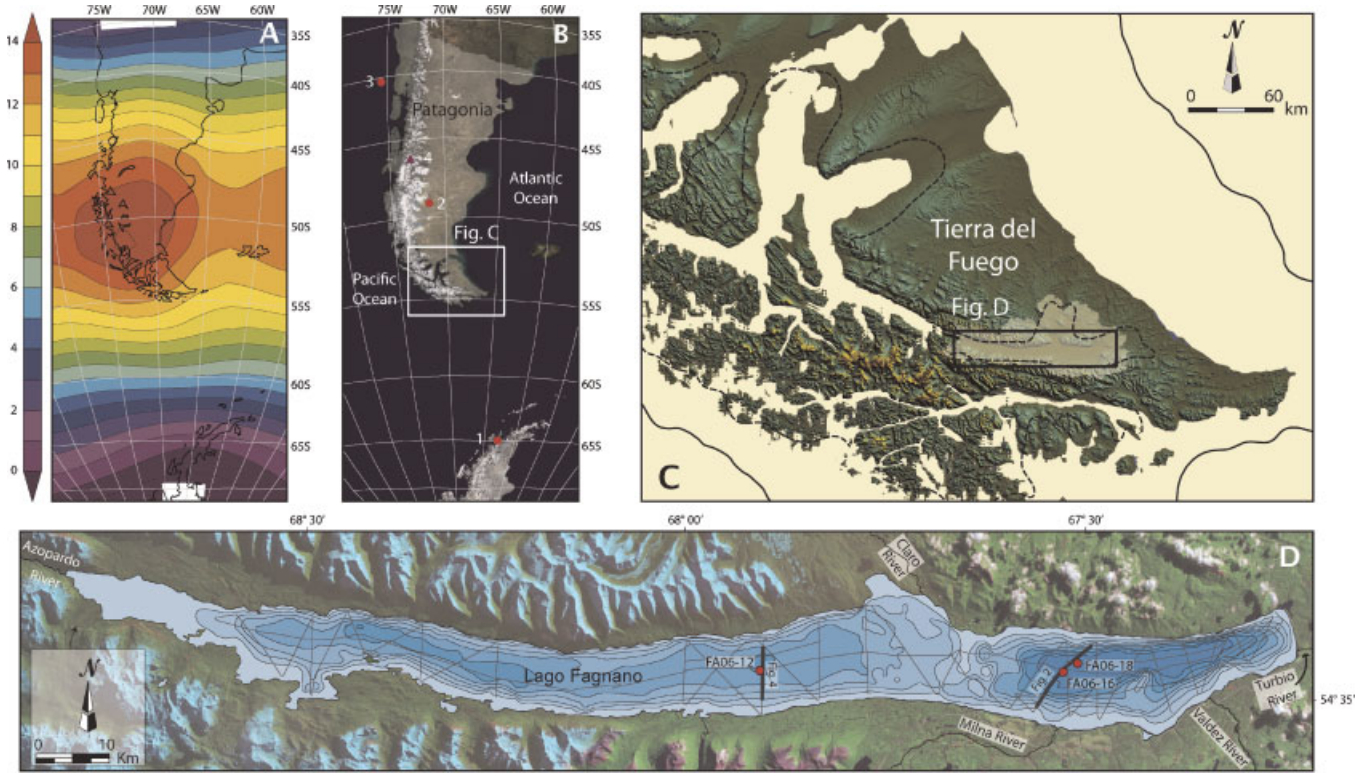

Figure 1 (A) 1000 mb zonal winds during the austral summer (December–January–February) over the Southern Hemisphere calculated for the time period from 1979 until 2005 (Kalnay *et al.*, 1996). Regional precipitation measurements are directly connected to these Southern Hemisphere westerlies. Note the increase values of zonal winds over southernmost Patagonia. (B) Satellite image of Patagonia and the sites cited in this paper: (1) the Palmer deep; (2) Lago Cardiel; (3) core GeoB 3313-1 offshore from Chile; (4) the Hudson volcano. (C) High-resolution digital elevation model (Mercator projection) from processed National Aeronautics and Space Administration (NASA) Shuttle Radar Topography Mission data (SRTM; Farr *et al.*, 2007) of Tierra del Fuego, with the watershed of Lago Fagnano shaded white. The dashed line marks the maximum extension of ice during the LGM (Coronato *et al.*, 2005) and a continuous line stands for the coastline (Rabassa *et al.*, 2000). (D) Bathymetric map of Lake Fagnano with a 25 m contour interval (modified from Lodolo *et al.*, 2003), showing the entire seismic grid. Thicker lines and solid dots indicate the location of the seismic profiles and sedimentary cores presented in this article

DOI: 10.1002/jqs

the lake indicate ongoing tectonic activity (Menichetti *et al.*, 2001; Ghiglione and Ramos, 2005). Moreover, fluvial drainages in the same region are clearly influenced by the presence of E–W striking structures related to the strike-slip fault system (Menichetti *et al.*, 2001).

Methods

The first seismic and coring campaigns on Lago Fagnano were carried out in 2005 and 2006 with the RV *Neecho*. Coring and seismic acquisition were restricted to the Argentinean portion of the lake, which is approximately 87% of the total lake surface area. The seismic survey comprised a ~800 km long grid of both single-channel high-resolution 3.5 kHz (pinger) and 1 in^3 (airgun) multichannel seismic data (Fig. 1(D)). Seismic profiles were digitally recorded in SEG-Y format, using a non-differential global positioning system (GPS) with an average accuracy of ±5 m. Processing of pinger data was carried out by bandpass filtering (2–6 kHz) and gaining with automatic gain control (AGC; window length 100 ms). Airgun data were also bandpass filtered (200–1000 Hz) and gained (AGC of 200 ms). Constant shallow noise was digitally removed and a water bottom mute was applied. The seismic data were interpreted at the University of Geneva using the Kingdom Suite™ software developed by Seismic Micro-Technology Inc. For calculation of velocity analyses, an average water column velocity of 1500 m s^{-1} was assumed.

Based on the seismic data interpretation, a series of 18 piston cores up to 8 m in length were recovered using a Kullenberg-type coring system. All cores were scanned before opening at ETH Zurich with a GEOTEK™ multisensor core logger (MSCL) to obtain their petrophysical properties (magnetic susceptibility, wet bulk density and P-wave velocity). The cores were subsequently opened, photographed, described and sampled for further sedimentological, geochemical and isotopic analyses. Composite sections were established using both short gravity cores that captured the sediment–water interface and long cores for the deeper subsurface sediments. Correlation between distinctive packages of laminae allowed building a composite section. Elemental determination at 0.3–0.7 mm resolution was carried out at the University of Geneva with a non-destructive Röntgenanalytik Eagle II X-ray microfluorescence (μ-XRF) system. The Rh tube acquisition parameters were set at 40 kV and 800 mA. The percentage of total organic carbon (TOC) was measured in dried powdered samples with a Rock-Eval (Re6) analyser at the University of Neuchâtel. Visual analyses of the sediments in smear slides were complemented by the use of a JEOL JSM-6400 scanning electron microscope at the University of Geneva. Radiocarbon dating was performed on terrestrial organic material found in a core retrieved in the western sub-basin using the AMS ^{14}C method (for details of radiocarbon methodology see Bonani *et al.*, 1987).

Seismic sequence stratigraphy

Acoustic penetration by the multichannel seismic system allowed identification of a complex bedrock morphology overlain by a thick sedimentary infill succession. While the entire sedimentary record reaches more than 100 m thickness in the eastern basin, it only reaches 60 m in the western basin (Figs. 2(A) and 3(A), respectively). This thickness discrepancy suggests either different sedimentation rates in the sub-basins or a longer temporal record in the east. In a forthcoming paper, we combine the deeper/older seismic stratigraphy, bathymetry and core sedimentology to identify a series of moraine complexes and use these data to reconstruct the deglacial history of the Fagnano lobe during the Lateglacial. Whereas the 1 in^3 airgun system provides enhanced visualisation of the deeper parts of the basin, the 3.5 kHz pinger seismic data provide high-resolution imaging for the shallower sedimentary record, which is the focus of this paper.

A seismic stratigraphic analysis of the pinger data from the eastern sub-basin allows the identification of three major stratigraphic units distinguished by different seismic facies: EA, EB and EC, from bottom to top (Figs. 2(B) and 3(B)). The seismic stratigraphy of this easternmost sub-basin as described in this paper follows the architecture previously described in detail by Waldmann *et al.* (2008) (units A–C). The seismic stratigraphy is characterised by a thick transparent chaotic unit (unit EA), followed by a series of transparent subunits separated by almost equally spaced continuous medium- to high-amplitude reflections (unit EB) and topped by intercalations of thinly spaced, high-amplitude internal reflections with low-amplitude to transparent intervals (unit EC). Unit EA has been interpreted to represent glacially derived sediments, while overlying unit EB is interpreted as fining upward sequences of proglacial turbidites, following a Swiss approach for investigation of perialpine lakes (Lister *et al.*, 1984). Unit EC contrasts sharply and represents a major environmental change with the onset of a pelagic-style sedimentation intercalated with sequences of downslope mass-flow events.

The seismic facies succession on the 3.5 kHz data of the western sub-basin exhibits a different pattern and does not follow the same architecture as the one in the eastern sub-basin. Thus the seismic stratigraphy for the western sub-basin is reconstructed independently with different names for the seismic units. As in the eastern sub-basin, we also recognise here three seismostratigraphic units, named WA–WC, from bottom to top (Fig. 3(B)). Only the top of unit (WA) is visualised by the 3.5 kHz data, while the base is beyond seismic penetration. Reflections within seismic unit WA are identified up to 10 m below the unit's top, before the reflected energy of the 3.5 kHz signal fades. Unit WA comprises a package of low-amplitude reflections with medium continuity topped by a semi-transparent and irregular subunit (Fig. 3(B)). The entire unit thickens slightly towards the depocentre. The overlying seismostratigraphic unit (WB), in contrast, is characterised by thinly spaced, high-amplitude reflections that gradually become lower in amplitude towards the top of the unit. Unit WB averages ~12 m in thickness and drapes the morphology of the lower unit. The youngest seismic unit (WC) is characterised by low-amplitude reflections occasionally intercalated with few semi-transparent intervals and medium- to high-amplitude internal reflections in the middle of the unit. Overall, unit WC reaches ~5 m thick and it mostly drapes the inherited topography. The seismic sequences and seismic facies were calibrated using the petrophysical properties and sedimentary record of two long cores, as described in the following sections.

Petrophysical, sedimentological and geochemical results

Both cores were subdivided into lithological units on the basis of sedimentology. These lithological units do not necessarily

DOI: 10.1002/jqs

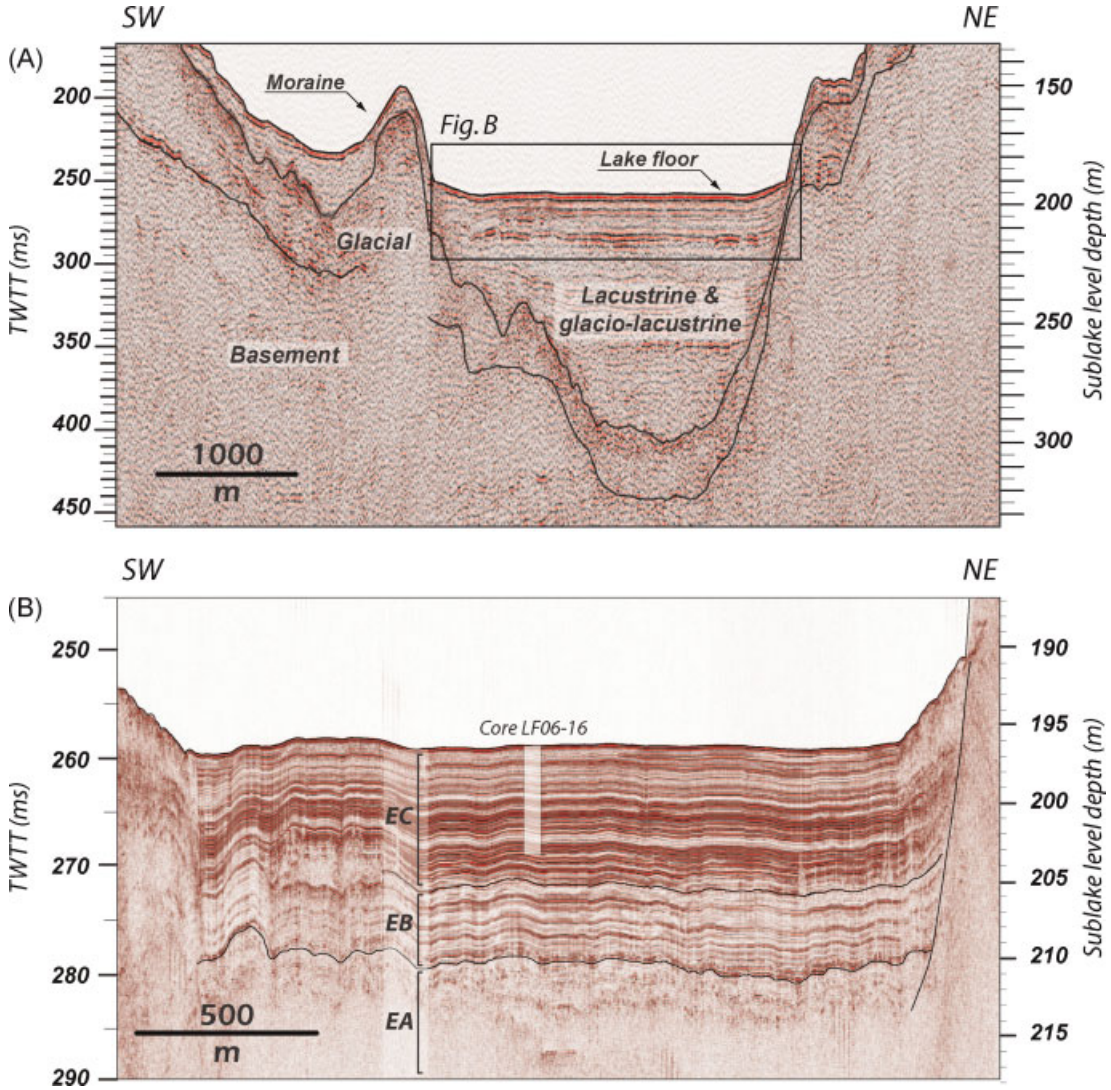

Figure 2 SW–NE transverse seismic profiles at the eastern sub-basin, showing the multichannel seismic profile (above) and the 3.5 kHz single-channel profile (below). Depth is given in both milliseconds of two-way travel time (TWTT) and consequently converted to sub-lake level depth (m) based on a P-wave velocity of 1500 m s^{-1} for water and sediment. The location of core LF06-PC16 is highlighted. Note the vertical scale exaggeration in the single-channel profile. This figure is available in colour online at wileyonlinelibrary.com

correlate between the basins and are independent of the seismic sequences.

Piston core LF06-PC16: eastern sub-basin

Piston core LF06-PC16 (in the eastern sub-basin) was retrieved at a water depth of 196 m, penetrating almost all seismic sequence EC and recovering almost 7.5 m of lacustrine sediments (Figs. 2(B) and 4). The sediment–water interface was recovered with this long core, and therefore we did not include a composite section with a short gravity core. Two lithological units are recognised in this core: the lowermost 60 cm correspond to lithological unit E1 whereas the reminder of the sedimentary record belongs to the younger lithological unit E2. Lithological unit E1 consists of alternating pale-brown silty clay to clay with 0.5–1.0 cm thick laminations. Lithological unit E2 consists entirely of uniform alternations of brown silty clay laminae with thin, 0.5–2.0 mm thick, dark-green to black, clay-enriched laminae. The dark lamination faded away immediately upon core opening, most likely indicating the presence of iron hydroxides. While diatoms, Fe and Mn dominate the dark-green laminae, Ca, Ti and K and fewer diatoms characterise the intercalated brownish clay laminae (μ-XRF analysis, as reported in Waldmann *et al.*, 2008). Amorphous organic matter is also a common component of the dark-green laminae. Moreover, vivianite was found sporadically disseminated throughout the sedimentary core which, once exposed to the ambient air, oxidised and consequently darkened to dark blue. This diagenetically formed mineral is generally found in organic-rich deposits with low rates of oxygen replacing organic material (Postma, 1981).

The sedimentary record is frequently interrupted by 3–15 cm thick, light-brown, graded layers composed of fine sand, silt and clay with relatively high magnetic susceptibility values interpreted as turbidites. Similar sequences were previously recognised on exposed lacustrine sediments surrounding Lago Fagnano (Bujalesky *et al.*, 1997). Variations in the petrophysical properties measured in core LF06-PC16 generally match the seismic reflection pattern of the penetrated units, allowing a precise core-to-seismic correlation. In a broad spectrum, bulk density and magnetic susceptibility values equally increase down-core. Small variations in both petrophysical values, however, appear closely associated with internal lithological changes mostly related to the presence of turbidites. Never-

DOI: 10.1002/jqs

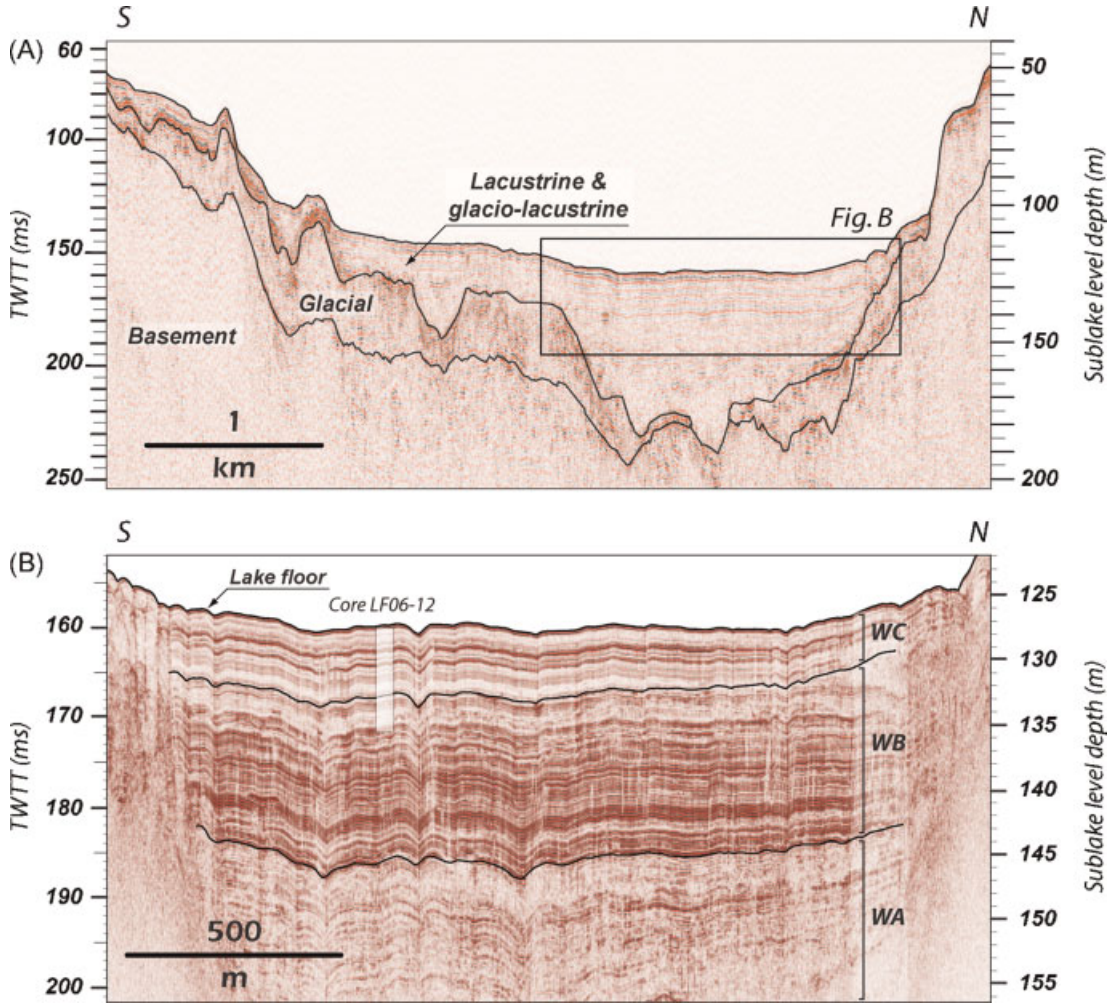

Figure 3 N–S transverse seismic profiles at the western sub-basin, showing the multichannel seismic profile (above) and the 3.5 kHz single-channel profile (below). Depth is given in both milliseconds of two-way travel time (TWTT) and consequently converted to sub-lake level depth (m) based on a P-wave velocity of 1500 m s^{-1} for water and sediment. The core LF06-PC12 setting is highlighted (see Fig. 1 for location). Note the vertical scale exaggeration in the single-channel profile. This figure is available in colour online at wileyonlinelibrary.com

theless, very high magnetic susceptibility values, such as those that occur at 4.8 m depth, correspond to a tephra layer identified in the sedimentary record. The petrophysical parameters commonly match as well the internal seismic architecture of the penetrated units, allowing a precise core-to-seismic correlation. These prominent petrophysical layers are linked to high-amplitude reflections in the seismic profile (Fig. 4). A general down-core decreasing TOC content is observed throughout the sedimentary core from values as high as 1.4% in the younger deposits toward low values of 0.4% in the older sediments. The μ-XRF-based iron content of the sedimentary sequence recovered in LF06-PC16 shows a general down-core increase from ~3 counts per second (cps) to 5 cps, coinciding with a gradual change from lithological unit E2 to E1.

Piston core LF06-PC12: western sub-basin

Core LF06-PC12 was retrieved at a depth of 127 m and recovered 7.5 m of lacustrine deposits, penetrating the entire seismic sequence WC and the uppermost part of WB (Figs 3(B) and 5). A composite section with short core FA05-3 was defined, since the sediment–water interface was not recovered in the long core. Four lithological units (W1–W4) are identified in this core; the oldest sediments of lithological unit W1 and W2 coincide with the top of seismic sequence WB; the entire WC sequence is recovered by lithological units W3 and W4. Lithological unit W1, at the core's base, is 20 cm thick, consisting of ~1–1.3 cm thick laminated light-brownish clay with relatively low bulk density and magnetic susceptibility values (Fig. 5). Overlying unit W2 has a thickness of 2.5 m and consists of 2–3 mm thick brown clay laminae alternating with slightly coarser and lighter-coloured laminae of clay and silt. Some 1–2 cm thick well-rounded clasts of plutonic origin are found within the laminae at the top of this unit. Higher in the stratigraphic succession, lithological unit W3 is a 3 m thick, 1–1.3 cm laminated, light-brown and mostly homogeneous clay. Bulk density values are fairly homogeneous and reach the highest levels during this sequence. The uppermost 2 m of the composite section corresponds to lithological unit W4, which consists of alternating fine black and brownish laminae, strongly resembling the lithological pattern previously described for unit E2 of core LF06-PC16. As in the eastern sub-basin, the sedimentary succession is interrupted by graded layers of fine sand to clay of 5–10 cm thickness representing turbiditic events (such as those high magnetic susceptibility values at 2 m and 2.6 m). Nevertheless, they appear less frequent in this sedimentary record than in the eastern sub-basin. An ash layer was recognised at a depth of 1.4 m in association with very high magnetic susceptibility values.

DOI: 10.1002/jqs

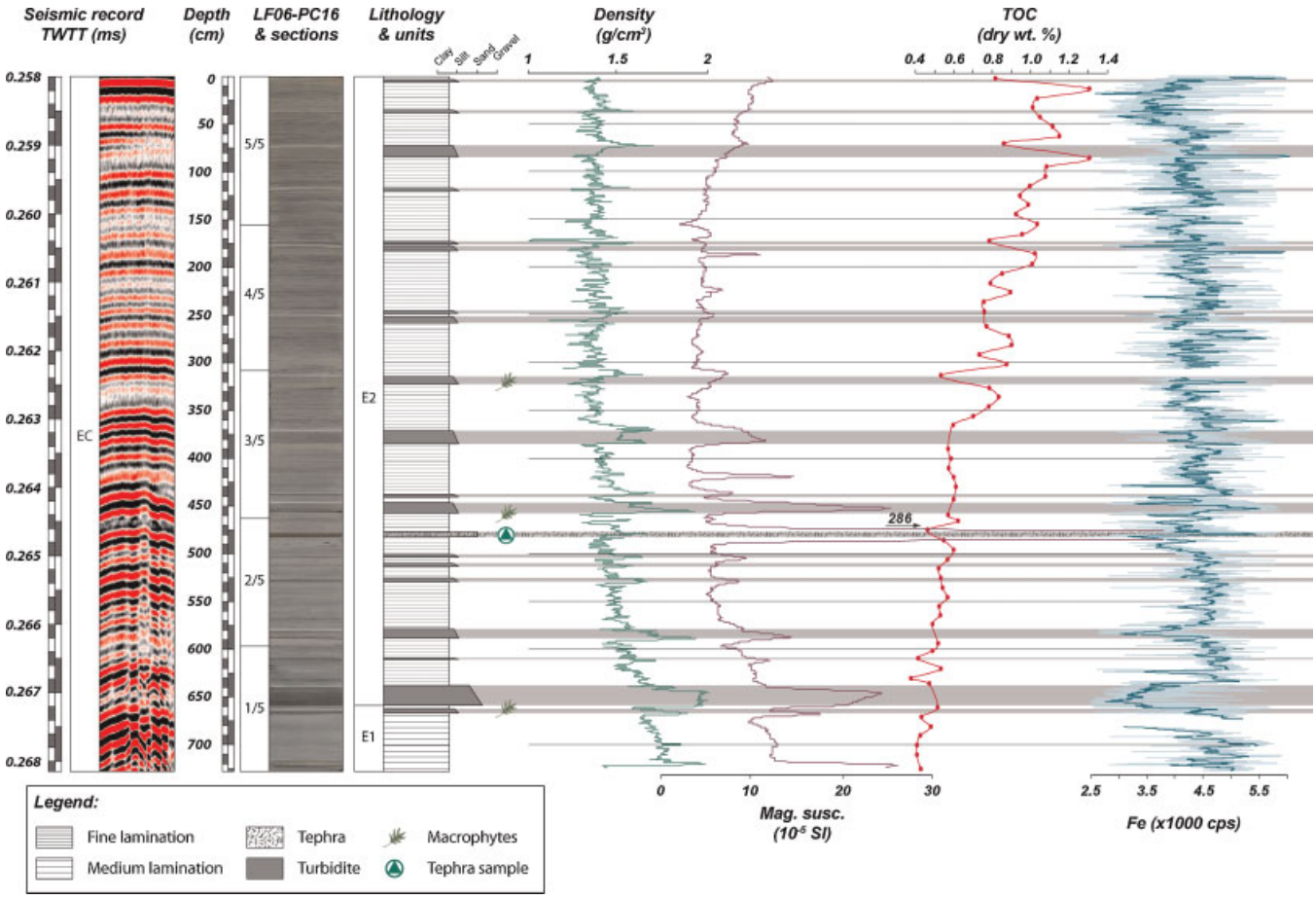

Figure 4 Petrophysical (bulk density and magnetic susceptibility), total organic carbon (TOC) and iron content data for piston core LF06-PC16. See text for further details. This figure is available in colour online at wileyonlinelibrary.com

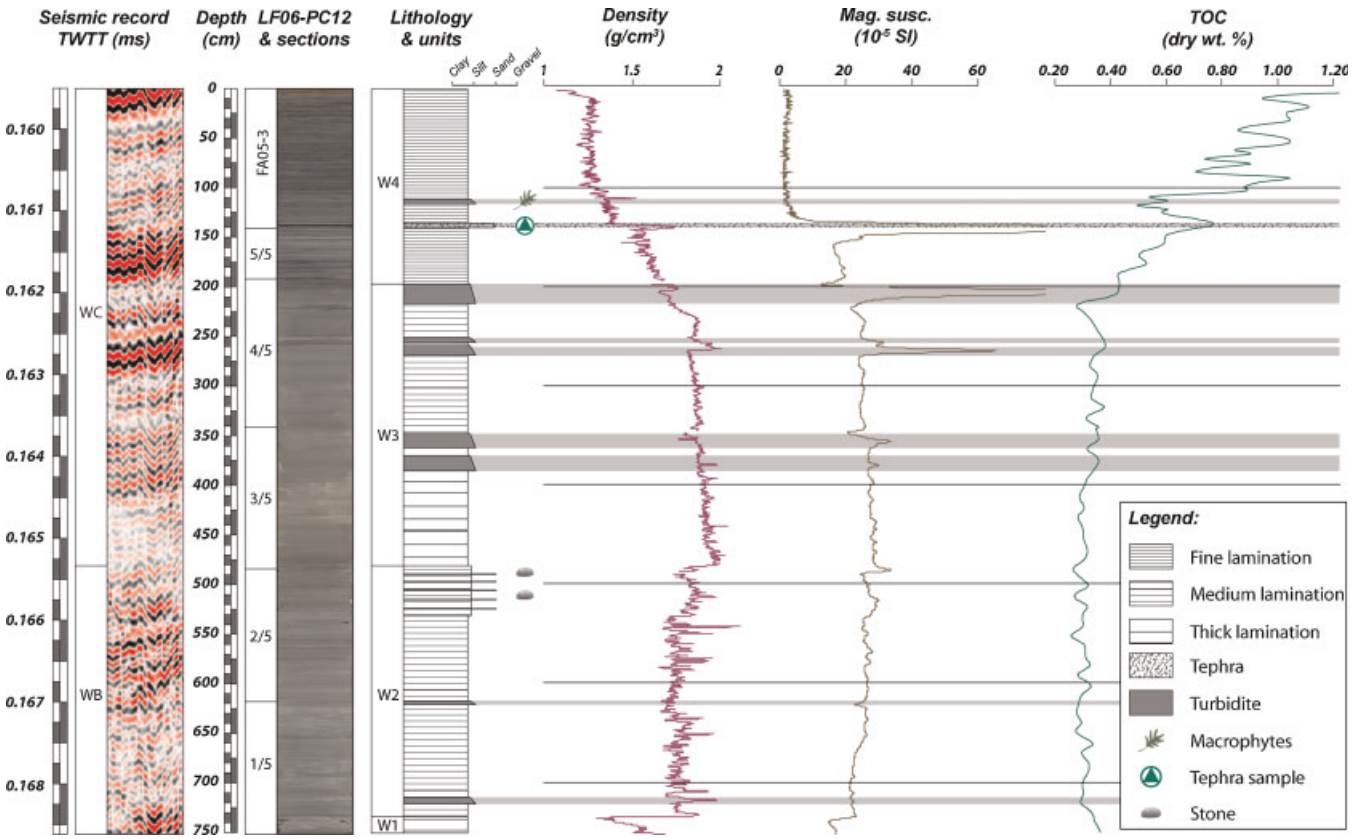

Figure 5 Petrophysical (bulk density and magnetic susceptibility) and total organic carbon (TOC) data for composite core LF06-PC12. See text for further details. This figure is available in colour online at wileyonlinelibrary.com

DOI: 10.1002/jqs

In general, both the bulk density and magnetic susceptibility increase down-core until 2.5 m depth. Further below, both parameters remain constant until they drastically diminish in lithological unit W1. TOC content shows a different trend, with decreasing values from ~1.3% to 0.3% in lithological unit W4 and constant values of 0.3%, with minor fluctuations throughout the rest of the core.

Core chronology

Tephrochronology

The appearance of tephra layers in the sedimentary record is an extraordinary advantage in performing tephrochronological analysis (e.g. Haflidason *et al.*, 1995). The tephra layers reveal distinctive petrophysical characteristics relative to the enclosing lacustrine sediments, making them excellent chronostratigraphic markers for a precise correlation among the cores and with seismic data. The different tephra levels were sampled and petrologically examined to reference the volcanic source material (Fig. 6). Moreover, the shards of both tephra layers were geochemically fingerprinted to confirm their origin (Table 1). The dark-green tephra layer at 140 cm and 480 cm in cores LF06-PC12 and LF06-PC16, respectively, consists of shards of green vesicular volcanic glass (<1 mm in size) along with a small proportion of plagioclase, orthopyroxene and clinopyroxene grains. In these respects it is petrologically equivalent to the characteristically green mid Holocene tephra H1, derived from the Hudson volcano (Fig. 1(A)), which occurs in Holocene deposits at numerous sites on Tierra del Fuego (Stern, 2008). Therefore we identify the tephra layers in both cores as one explosive event, the Hudson H1 ash, dated to 6700 ± 65 ^{14}C a BP (7570 +110/−140 cal. a BP) (Naranjo and Stern, 1998; Stern, 2008).

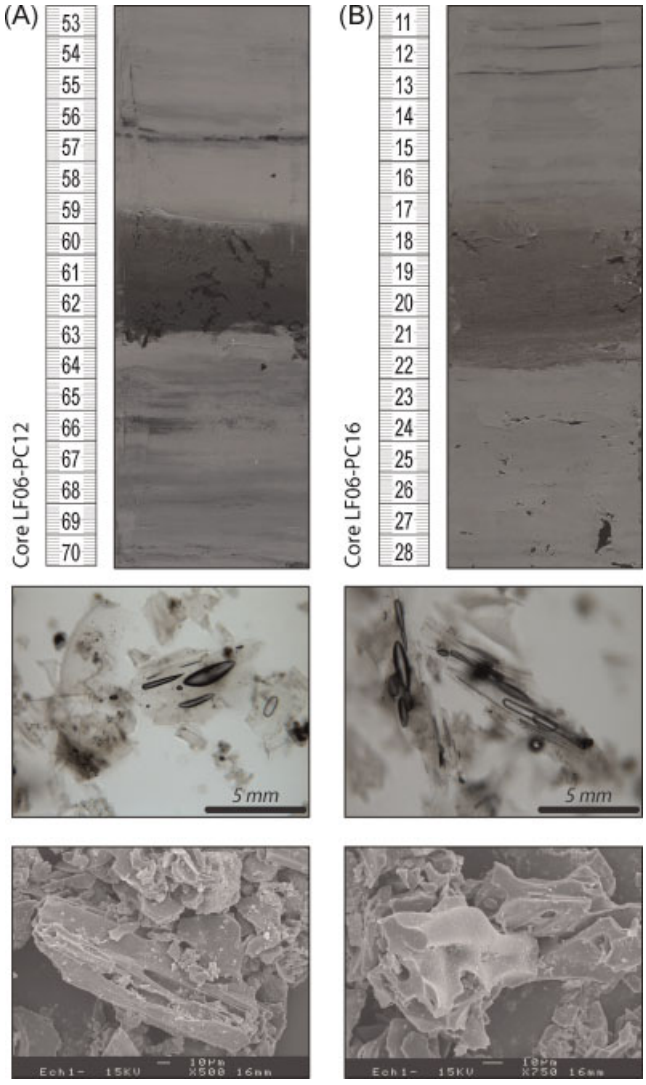

Figure 6 Macroscopic, microscopic and scanning electron microscope images of the tephra layers in core LF06-PC12 (on the left, A) and core LF06-PC16 (on the right, B). The similarity between the morphology and structure of the shards among both cores indicates the Hudson H1 explosion at 7570 cal. a BP as the source event for the three ash levels. This figure is available in colour online at wileyonlinelibrary.com

Table 1 Geochemical composition of the tephra layers found in Lago Fagnano cores. The results are compared with data from Naranjo and Stern (1998) showing similar geochemical properties and thus indicating the source of the shards as the Hudson H1 explosive event. Data obtained by measurements at the University of Colorado at Boulder. [a]–data obtained from Naranjo and Stern (1998).

Sample no.: Material:	LF06-PC12 Tephra	LF06-PC16 Tephra	94T-44[a] Pumice	TDF[a] Tephra
Ti	8422	8649	9112	8513
Mn	1240	1323	1340	1085
Cs	1.3	1.4	1.3	1.3
Rb	49	52	47	53
Sr	377	380	382	369
Ba	800	807	797	852
Y	41	41	38	41
Zr	355	361	338	365
Nb	16	17	14	16
Hf	10.0	9.5	10.3	9.5
Ta	1.8	1.5	n.a.	n.a.
Pb	12.6	13.2	n.a.	n.a.
Th	6.5	6.3	6.8	6.4
U	1.2	1.2	n.a.	n.a.
La	39.9	40.3	41.3	37.5
Ce	85.2	81.2	85.9	78.3
Pr	9.7	9.7	n.a.	n.a.
Nd	42.3	42.7	43.1	40.9
Sm	8.62	8.66	8.58	n.a.
Eu	2.41	2.41	2.43	2.23
Gd	10.6	10.8	n.a.	n.a.
Tb	1.29	1.26	1.25	1.17
Dy	7.53	7.95	n.a.	n.a.
Ho	1.48	1.43	n.a.	n.a.
Er	4.50	4.74	n.a.	n.a.
Tm	0.58	0.56	n.a.	n.a.
Yb	4.28	4.39	4.71	4.19
Lu	0.61	0.65	0.70	0.61

Radiocarbon

Two radiocarbon ages were obtained from terrestrial material retrieved in the sedimentary record of core LF06-PC16 (Table 2). The radiocarbon ages fall in agreement with the depth of the H1 tephra. The age model is thus defined for core LF06-PC16 combining both the radiocarbon and tephrochronology data.

DOI: 10.1002/jqs

Table 2 Radiocarbon and calibrated ages retrieved from cores in the eastern lake sub-basin. Tephra age was obtained from Stern (2008). Calibration was calculated using the web-based *CalPal* shareware converter tool (http://www.calpal-online.de/)

Sample	Lab. no.	Depth (cm)	Dated material	^{14}C age (a BP)	^{13}C (‰)	Cal. age (a BP)
PC16-C15	ETH-35343	318	Wood	5 445 ± 125	−20.3	6 213 ± 149
PC16-C23	ETH-35453	612	Wood	10 435 ± 75	−28.4	12 358 ± 149
PC16-T1		480	Tephra	6 850 ± 150	n.a.	7 570 ± 120

Discussion

Sedimentological and palaeohydrological implications

Interpretation of the seismic architecture shows a tectonoglacial origin of the Lago Fagnano basin that was gradually filled up by glacially derived and lacustrine sediments, which occasionally intercalate with deposits resulting from mass wasting events such as turbidites (Waldmann *et al.*, 2008). This sequence represents a typical succession of a glacial fjord-like elongated basin as seen in similar lacustrine settings such as in the Finger Lakes region (Mullins *et al.*, 1996), in the Alps (van Rensbergen *et al.*, 1999; Chapron *et al.*, 2002) and in the Andes (Charlet *et al.*, 2008).

The contrasting depths of the H1 tephra in both eastern and western cores suggest substantial differences in sedimentation rate in both sub-basins. In the eastern sub-basin it is calculated as 0.63 mm a^{-1} for core LF06-PC16. This calculation includes turbidite layers, which increase the pure background sedimentation rate. In this distal location in the basin centre, turbidites are not expected to erode the underlying beds substantially; consequently we simply subtract the major turbidites from the sedimentary column in order to calculate the background sedimentation rate of 0.50 mma^{-1}. Performing the same calculation on the uppermost part of core LF06-PC12 for the western sub-basin, the background sedimentation rate decreases to 0.2–0.3 mm a^{-1}.

The tephra layer found in both cores and dated as ∼7500 cal. a BP separates the sedimentary sequence approximately into a younger section high in organic content and an into an older, organic-depleted sequence (Fig. 7). The cyclic alternation of brown clay and black organic-enriched laminae, which typifies most of core LF06-PC16 (seismic sequence EC) and the upper part of core LF06-PC12 (seismic sequence WC), suggests sedimentation in a well-stratified lake with high TOC content but no bioturbation, as is seen in similar alpine lacustrine environments (Ariztegui *et al.*, 1996). This interpretation is supported by the sporadic presence of vivianite, which is usually formed in organic-rich environments under anoxic or dysoxic conditions at the sediment–water interface (Postma, 1981). As seen on seismic data, this pelagic style of sedimentation resulted in a draping geometry and occurred in a basin that was no longer in direct contact with the glacier, as is known from similar Holocene successions in former Alpine proglacial lakes (e.g. Girardclos *et al.*, 2005). We suggest that the lower lithological units of core LF06-PC12, which hold very low organic content, most probably represent periods of high detrital input, particularly during the early Holocene retreat of the Fagnano glacier. This assumption is supported by the occurrence of small well-rounded clasts in the laminated sequence of lithological unit W2, which we interpret as dropstones from icebergs calving from the retreating glacial front. This finding implies that during the depositional period of lithological units W1 and W2 at least the western part of Lago Fagnano was a proglacial lake in physical contact with the glacier's tongues. Furthermore, accumulation of ice-rafted debris may represent increased calving of icebergs from the Fagnano glacier.

The background sedimentation rate discrepancy between both sub-basins is probably caused by differential changes in the sediment supply to the lake since the Lateglacial. During the time interval covered by the lithological units below the tephra layer (primarily units W1, W2, W3 and E1) a radical change occurred in the hydrology and water circulation of the lake. The main supplier of sediment to the lake basin during this period was the Fagnano glacier and its tributaries, which were located somewhere at the eastern basin and probably blocking the outlet to the Admiralty Sound and the Magellan Strait. This is mainly evidenced by the occurrence of dropstones in core LF06-PC12. During this period the lake's waters were emptied towards the Atlantic Ocean, as is also recorded by fluvial outwash relics in the San Pablo River east of Lago Fagnano (Coronato *et al.*, 2005). Once the glaciers retreated, however, the passage to the Pacific Ocean was opened and the lake's internal hydrology overturned, establishing the present drainage pattern. We further propose that the sedimentation rate differences may probably be related to the position of the morphological sill as a major divide between both sub-basins. During the period of western sediment supply by the glacier, the westernmost sub-basin was the main morphological receptacle of clastic material. However, the situation changed thereafter when the easternmost sub-basin became the main sediment receptacle with the onset of eastern fluvial clastic supply. Thus, we propose that the combination of inherited basal morphology, the glacier's retreats and hydrological changes in the lake resulted in different temporal sedimentation rates between both sub-basins.

The total sedimentation rate (which includes the presence of turbidites in the record) also varies between both sub-basins. The eastern sub-basin is deep with low-angle edges (∼40–45°) that promote slope sedimentation and subsequent remobilisation downslope. This architecture is likely triggered by seismic events along the MFT in a process that was also recognised in other Alpine lacustrine settings (e.g. Chapron *et al.*, 1999; Schnellmann *et al.*, 2005; Fanetti *et al.*, 2007; among others). In contrast, the basal morphology of the western sub-basin shows high-angle (∼60°), narrower shoulders preventing downslope sediment deposition and thus fewer downslope remobilisation events. These differences explain the frequency of turbidite events in both basins. Sedimentation rates may also vary within each sub-basin as a consequence of the distance to the sedimentary source.

Palaeoclimate Implications

To ensure that the observed changes at 54° S in Lago Fagnano reflect widespread climate variations in the Southern Hemisphere, we compared our findings with Holocene marine and

DOI: 10.1002/jqs

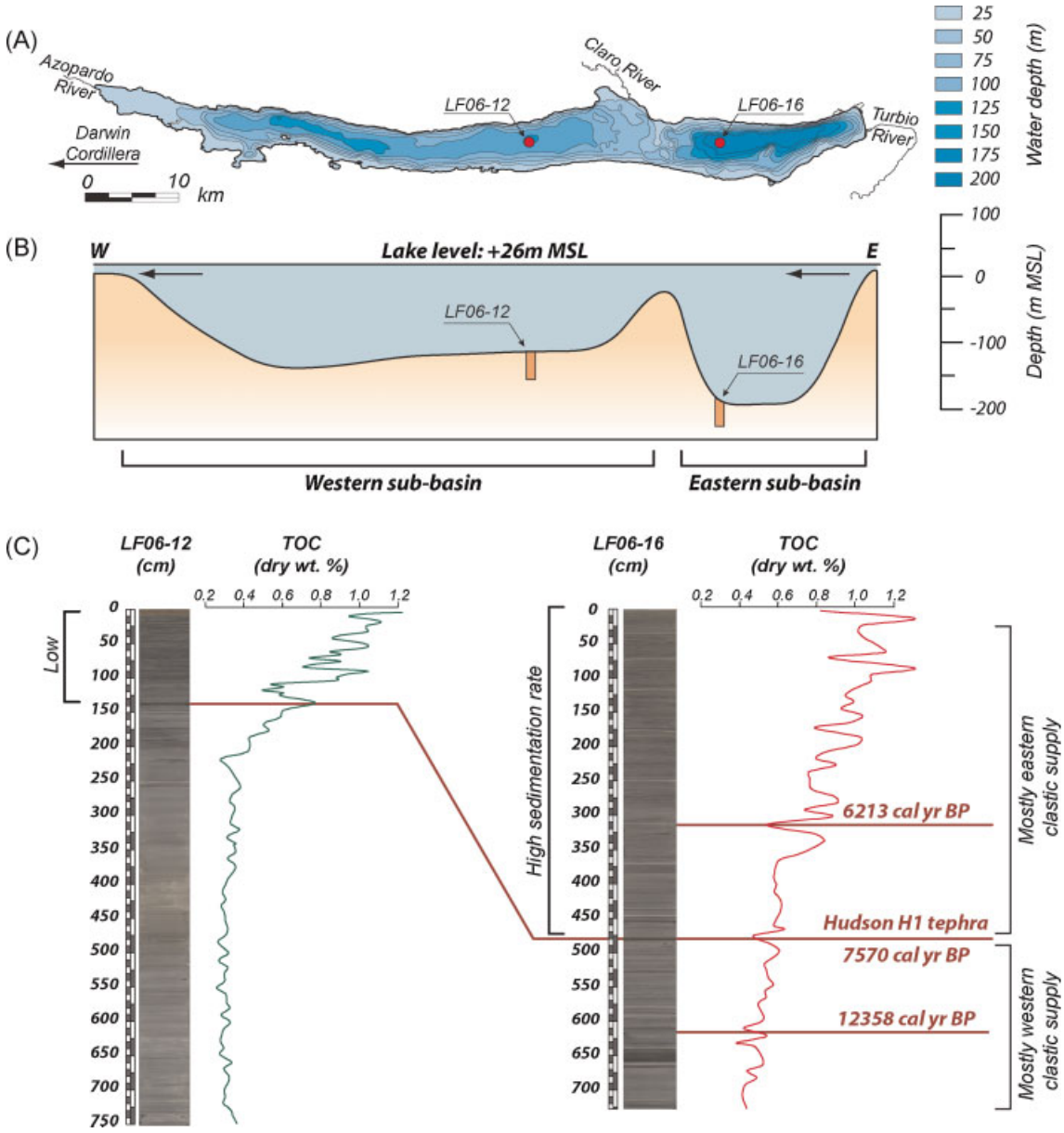

Figure 7 A palaeohydrological model of Lago Fagnano. (A) The bathymetry and core locations sited in this paper. (B) A simplified E–W morphological cross-section of Lago Fagnano with core locations. (C) Cores LF06-PC12 and LF06-PC16 with TOC content and correlation through the tephra layer. Note the variations in the interpreted clastic supply to the lake above and below the tephra layer and discrepancies in the sedimentation rate. See text for further details. This figure is available in colour online at wileyonlinelibrary.com

continental palaeoclimate records as well as with temperature proxies from Antarctic ice cores and they are further explained therein. The sedimentary record of core LF06-PC16 from Lago Fagnano is chronologically framed by both the H1 tephra layer and two radiocarbon samples enabling us to perform such a comparison of climate proxies with other regional records. The turbidite layers were removed from the petrophysical and geochemical data, allowing a depth correction.

The Hypsithermal Interval

The Hypsithermal period (or Holocene climatic optimum) in Southern Patagonia (ca. 9–6 cal. ka BP) is characterised by a weakened influence of the polar maritime air fronts and by a warming trend that produced a climate much warmer and drier than present (McCulloch *et al.*, 2000).

The iron content trend line of core LF06-PC16 from Lago Fagnano is presented in Fig. 8(A). We have removed the turbidites from this profile in order to eliminate the tectonic/mass wasting influence and focus on the palaeoclimate record. This proxy represents variability in the detrital magnetic minerals (e.g. magnetite) input to the basin that is further controlled by changes in precipitation in the watershed. Oscillations in the iron content trend are thus indirectly related to variability in precipitation, similarly to other Patagonian settings (e.g., Haberzettl *et al.*, 2005). From the deepest intervals of the record towards the early Holocene H1 tephra, the Fagnano iron content during the Hypsithermal shows a declining trend that culminates proximal to the H1 tephra. Superimposed on this trend are a series of significant oscillations ranging between 4500 and 3000 cps. The trend in iron content may be related to drier conditions in the Fagnano watershed that limited the amount of runoff entering the lake. The timing of aridity is generally consistent with previous climate model reconstructions for the Fuegian archipelago, such as from palynology studies in peat deposits (Borromei, 1995; Unkel *et al.*, 2008) and in glacial deposits (Heusser, 1998). The iron content record from Lago Fagnano,

DOI: 10.1002/jqs

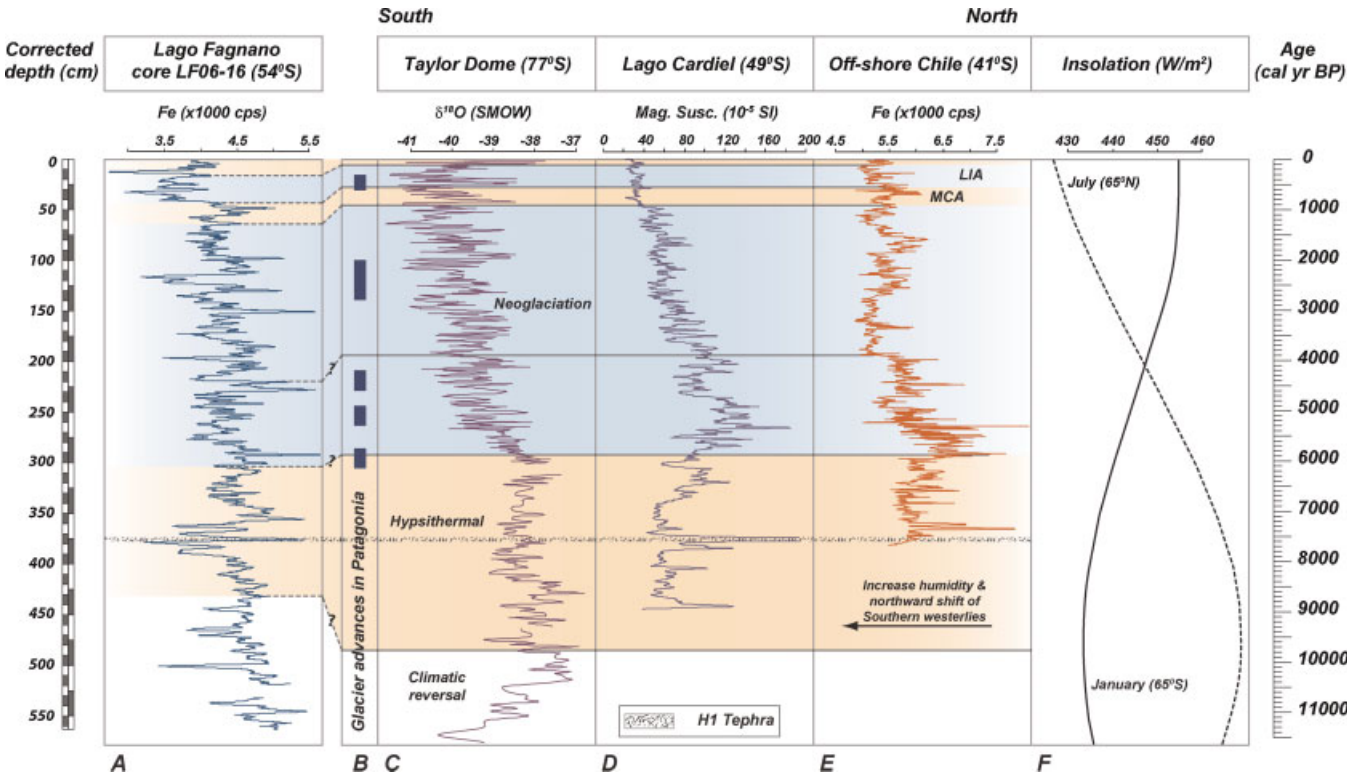

Figure 8 Comparison among Lago Fagnano data with other regional datasets plotted in an S–N transect. (A) Iron content record from core LF06-PC16 in Lago Fagnano without the turbidite layers values and corrected depth. (B) Timing of main glacier advances in southern Patagonia (Porter, 2000; Douglass *et al.*, 2005). (C) Oxygen isotope record from Taylor dome, at 77° S in Antarctica (Steig *et al.*, 1998). (D) Magnetic susceptibility of core CAR 99-9P from Lago Cardiel at 49° S (Gilli *et al.*, 2005). (E) Iron content in a marine sedimentary core offshore Chile at 41° S (Lamy *et al.*, 2001). (F) July and January insolation curves for 65° N and 65° S, respectively (Berger and Loutre, 1991). The light shaded bars stand for substantial climatic periods, as recognised in Antarctica. The timing of the Hudson H1 tephra is highlighted to facilitate correlation with the Fagnano record. This figure is available in colour online at wileyonlinelibrary.com

however, falls out of phase with the magnetic susceptibility proxy recorded from Lago Cardiel at 49° S (Fig. 8(D)) (Gilli *et al.*, 2001). This out-of-phase relation suggests that, while drying conditions prevailed in Tierra del Fuego during the Hypsithermal, the more northern latitudes such as around Lago Cardiel, at 49° S, and offshore Chile, at 41° S (Lamy *et al.*, 2001) (Fig. 8E) experienced an increase in humidity likely caused by a local intensification of the Southern Westerlies winds (Gilli *et al.*, 2005) or easterly moisture (Markgraf *et al.*, 2003). The reconstructed climate record from Lago Fagnano compares well with the high-resolution marine record of the Holocene optimum at Palmer Deep (77° S) offshore from the Antarctic Peninsula (Domack *et al.*, 2001; Brachfeld *et al.*, 2002). However, the high amplitude of the climatic signal in the latter may be a positive feedback due to sea ice expansion and subsequent influence of ice rafting debris in the Southern Ocean.

The iron content trend of Lago Fagnano during the Hypsithermal period is consistent with the oxygen isotope record from the Taylor Dome ice core, at 77° S in Antarctica (Fig. 8(C)) (Steig *et al.*, 1998). Dry conditions and reduced westerlies at the latitude of Lago Fagnano (54° S) coincide with warmer air temperatures over the Antarctic continent, suggesting that the temperature gradient and the overall atmospheric circulation in the high southern latitudes was reduced at this time. By contrast, dominance of this wind belt has been a characteristic feature of later climate oscillations throughout the Neoglacial period. At ca. 5500 cal. a BP, renewed glacial activity in southern South America reflects a combination of wetter and/or cooler conditions as is recorded by glacier advances in Southern Patagonia (Clapperton and Sugden, 1988). Moreover, the transition from the Hypsithermal to the Neoglacial period is consistent with changes in summer insolation forcing at high latitudes (Fig. 8(F)) (Berger and Loutre, 1991). Considering the orbital parameters defining Earth's insolation, the seasonality contrast at high latitudes increased since the beginning of the Holocene (Kutzbach *et al.*, 1993), typifying the Southern Hemisphere with relatively warmer winter seasons and milder cooler summers than today.

The Neoglacial Interval

The onset of the Neoglacial period in Tierra del Fuego is represented by an augmentation in the iron content values (higher than 5000 cps) (Fig. 8(A)) and is interpreted as an increase in the sediment supply to the basin, which is most likely related to precipitation intensification in the lake watershed. Since moisture mainly arrives from the Pacific Ocean carried by the Southern Hemisphere westerlies, enhancement of rainstorm frequency is linked to intensification of the regional wind activity. A similar scenario was proposed for other Patagonian lakes at lower latitudes, such as Lago Guanaco at 51° S (Moy *et al.*, 2008), Lago Cardiel at 49° S (Gilli *et al.*, 2005) and Lago Puyehue at 40° S (Bertrand *et al.*, 2008). Evidence for humidity rise during the Neoglacial period is well recorded by four periods of significant glacier advances both in Patagonia and Antarctica that are dated to 5400–4900, 4700–4200, 2700–2000 cal. a BP and during the 15th to late 19th centuries AD (Fig. 8(B)) (Clapperton and Sugden, 1988; Kuylenstierna *et al.*, 1996; Porter, 2000; Kilian *et al.*, 2007). These Neoglacial glacier advances are also recognised in sites east of Tierra del

DOI: 10.1002/jqs

Fuego by an abrupt increase in ice-rafted debris at 53° S in the Southern Atlantic Ocean (Hodell *et al.*, 2001) and even at 37° S by vegetation dynamics in Nightingale Island (Ljung and Bjorck, 2008).

The high iron content values in the Fagnano record roughly follow similar patterns in the oxygen isotope record from Taylor Dome at 77° S in Antarctica (Fig. 8(C)) (Steig *et al.*, 1998) and in the iron content offshore from Chile at 41° S (Fig. 8(E)) (Lamy *et al.*, 2001), suggesting a latitudinal climate connection. This climatic relationship during the late Holocene, and the recognition of the Medieval Climate Anomaly (MCA) and the Little Ice Age (LIA) in the marine record offshore from Chile, encourage us to search for similar patterns in the Lago Fagnano record.

The MCA in Fagnano is recognised by low iron content intervals, interpreted to represent decreased precipitation coupled by glacier retreat. This pattern is further recognised in inland areas by pollen records in peat bogs (Mauquoy *et al.*, 2004). The LIA, however, shows an inverse trend with relative high iron content levels linked to the intensification of the Southern Westerlies and humidity increase. The latter is consistent with previously reported glacier advances in Tierra del Fuego (Planas *et al.*, 2002; Coronato *et al.*, 2005).

Latitudinal shifts of the Southern Hemisphere westerlies

Latitudinal shifts in the Southern Hemisphere westerlies have been proposed to occur since the Middle Holocene (Markgraf, 1993), although their position through time is still controversial (Lamy *et al.*, 1999; Jenny *et al.*, 2002; Markgraf *et al.*, 2003). The spatial and temporal interpolation of the different records allows us to propose a timeframe of the Southern Westerly wind belt strengthening at the latitude of the Island of Tierra del Fuego.

The southward migration of the Southern Westerlies is accompanied by a synchronous southward shift of the Antarctic Circumpolar Current (ACC) (Lamy *et al.*, 2002). This warming trend in the Southern Ocean sea-surface temperature during the Hypsithermal period and beginning of the Neoglacial indicates a decrease in advection of ACC-derived water masses, and thus an increase in the humidity in Southern Patagonia, as the Southern Westerlies migrated to these latitudes. The reconstructed iron content record from the high-resolution Pacific Ocean sedimentary core offshore from Chile at 41° S (Fig. 8(E)) shows fluctuations that are interpreted as a poleward shift of the Southern Westerlies wind belt already at around 5500 cal. a BP (Lamy *et al.*, 2001, 2002). Moreover, the magnetic susceptibility record from Lago Cardiel, which is located at 49° S (Gilli *et al.*, 2005) (Fig. 8(D)), shows similarities to the iron content in the marine record, but lagging for several hundreds years later. This relationship indicates that the Southern Westerlies wind belt migrated to these latitudes later in time. This link is strengthened by glacier advances at 6200 a evidenced at 46° S (Douglass *et al.*, 2005). Considering our proposed age model and assuming a constant sedimentation rate for Lago Fagnano, at least since the H1 ash layer, the highest iron content values recorded in core LF06-PC16 at the corrected depth of 3 m (without the turbidite layers; Fig. 8(A)) may have occurred ca. 5500–6000 cal. ka BP. This interval coincides with the onset of the Southern Westerlies and intensification of humidity in the region. We further propose that the relatively low iron content values at the corrected depth of 60–90 cm, which are followed by high iron content values at 50 cm depth, may indicate the onset of the MTA followed by the LIA in the Island of Tierra del Fuego.

These lines of evidence propose that the palaeoclimatological reconstruction from Lago Fagnano furnish more information related to the positioning of the Southern Westerlies wind belt in this region, providing additional data on the forcing mechanism behind climate change in the southernmost extreme of South America.

Conclusions

The Lago Fagnano record provides a unique view of hydrological and sedimentary changes caused by variability in the Southern Hemisphere westerly wind since the middle Holocene. These results indicate that:

1. The Hudson H1 ash (7570 +110/−140 cal. a BP (Stern, 2008) was identified in the Lago Fagnano record. The age of the sedimentary record was constrained by this chronostratigraphic marker spanning the entire Neoglacial and probably most of the Hypsithermal.
2. Magnetic susceptibility and total iron content in Lago Fagnano record climatic changes that are further correlated with other regional marine and continental climate archives. Our record shows fluctuations that are further interpreted as variations in humidity in Tierra del Fuego. Low magnetic susceptibility and iron content values typify the Fagnano record during the Hypsithermal period. Contrarily, an opposite tendency occurred during the Neoglacial associated with the onset of humid conditions in the region.
3. The onset of distinctive climate events during the Holocene, such as the MTA and the LIA, was recognised in the Island of Tierra del Fuego, by comparing the iron content record of Lago Fagnano with other records elsewhere. The MTA interval is identified as a diminution of the iron content related to regional drought, and is further recognised inland by other proxies. The onset of the LIA, however, is related to increase in the iron content interpreted as intensification of the regional humidity and coupled by substantial advances of regional glaciers.
4. Moisture changes at 54° S in Lago Fagnano are linked to variations in the positioning of the Southern Westerlies through time. The onset of this wind belt in the Island of Tierra del Fuego appears to occur later than at lower latitudes of mainland Patagonia.
5. Our palaeoclimatological reconstruction from Lago Fagnano can be related to the positioning of the Southern Westerlies wind belt. It provides additional information to constrain the timing and magnitude of known Holocene climate fluctuations in the southernmost extreme of South America.

Acknowledgements We acknowledge Stanford University for the use of its capable small vessel, the RV *Neecho*. We thank Steffen Saustrup and Mark Wiederspahn of the Institute for Geophysics, and David Mucciarone of Stanford, for technical assistance during all aspects of the fieldwork. Captains Jorge Ebling and Rafael Quezada are also kindly acknowledged for their help during fieldwork. The field expeditions could not have been accomplished without the assistance and logistic help of the Centro Austral de Investigaciones Científicas – Consejo Nacional de Investigaciones Científicas y Técnicas (CADIC-CONICET Argentina) and Prefectura Naval Argentina. The logistical help and hospitality of Alejandro, Maria Elena and Gabriel Echeverría from Bahía Torito are kindly acknowledged. We thank Thierry Adatte (University of Neuchâtel) for total organic carbon analyses. NCEP reanalysis of the zonal wind is provided by the NOAA/OAR/ESRL PSD at Boulder (CO, USA) from their website at http://www.cdc.noaa.gov/. This work is part

of the project Environmental Changes Down-South (ENDS), supported by the Swiss National Science Foundation grants 200021-100668/1 and 200020-111928/1. We also acknowledge support from the US National Science Foundation (RD) and the National Geographic Society (grant CRE 7705-04) (to JA).

References

Ariztegui D, Farrimond P, McKenzie JA. 1996. Compositional variations in sedimentary lacustrine organic matter and their implications for high Alpine Holocene environmental changes: Lake St Moritz, Switzerland. *Organic Geochemistry* **24**: 453–461.

Berger A, Loutre MF. 1991. Insolation values for the climate of the last 10 000 000 years. *Quaternary Science Reviews* **10**: 297–317.

Bertrand S, Charlet F, Charlier B, Renson V, Fagel N. 2008. Climate variability of southern Chile since the Last Glacial Maximum: a continuous sedimentological record from Lago Puyehue (40° S). *Journal of Paleolimnology* **39**: 179–195.

Bonani G, Beer J, Hofmann H, Synal HA, Suter M, Wolfli W, Pfleiderer C, Kromer B, Junghans C, Munnich KO. 1987. Fractionation, precision and accuracy in C-14 and C-13 measurements. *Nuclear Instruments and Methods in Physics Research Section B – Beam Interactions with Materials and Atoms* **29**: 87–90.

Borromei AM. 1995. Pollen analysis from a Holocenic peat in the valley of Andorra, Tierra de Fuego, Argentina. *Revista Chilena de Historia Natural* **68**: 311–319.

Brachfeld SA, Banerjee SK, Guyodo Y, Acton GD. 2002. A 13 200 year history of century to millennial-scale paleoenvironmental change magnetically recorded in the Palmer Deep, western Antarctic Peninsula. *Earth and Planetary Science Letters* **194**: 311–326.

Bujalesky GG, Heusser CJ, Coronato AM, Roig CE, Rabassa JO. 1997. Pleistocene glaciolacustrine sedimentation at Lago Fagnano, Andes of Tierra del Fuego, Southernmost South America. *Quaternary Science Reviews* **16**: 767–778.

Chapron E, Beck C, Pourchet M, Deconinck JF. 1999. 1822 earthquake-triggered homogenite in Lake Le Bourget (NW Alps). *Terra Nova* **11**: 86–92.

Chapron E, Desmet M, De Putter T, Loutre MF, Beck C, Deconinck JF. 2002. Climatic variability in the northwestern Alps, France, as evidenced by 600 years of terrigenous sedimentation in Lake Le Bourget. *The Holocene* **12**: 177–185.

Charlet F, de Batist M, Chapron E, Bertrand S, Pino M, Urrutia R. 2008. Seismic stratigraphy of Lago Puyehue (Chilean Lake District): new views on its deglacial and Holocene evolution. *Journal of Paleolimnology* **39**: 163–177.

Clapperton CM, Sugden DE. 1988. Holocene glacier fluctuations in South America and Antarctica. *Quaternary Science Reviews* **7**: 185–198.

Coronato A, Seppälä M, Rabassa J. 2005. Last glaciation landforms in Lake Fagnano ice lobe, Tierra del Fuego, southernmost Argentina. In *6th International Conference on Geomorphology*, Zaragoza.

Domack E, Leventer A, Dunbar R, Taylor F, Brachfeld S, Sjunneskog C, Party OLS. 2001. Chronology of the Palmer Deep site, Antarctic Peninsula: a Holocene palaeoenvironmental reference for the circum-Antarctic. *Holocene* **11**: 1–9.

Douglass DC, Singer BS, Kaplan MR, Ackert RPJ, Mickelson DM, Caffee MW. 2005. Evidence of early Holocene glacial advances in southern South America from cosmogenic surface exposure dating. *Geology* **33**: 237–240.

Fanetti D, Anselmetti FS, Chapron E, Sturm M, Vezzoli L. 2007. Megaturbidite deposits in the Holocene basin fill of Lake Como (Southern Alps, Italy). *Palaeogeography, Palaeoclimatology, Palaeoecology* **259**: 323–340.

Farr TG, Rosen PA, Caro E, Crippen R, Duren R, Hensley S, Kobrick M, Paller M, Rodriguez E, Roth L, Seal D, Shaffer S, Shimada J, Umland J, Werner M, Oskin M, Burbank D, Alsdorf D. 2007. The shuttle radar topography mission. *Reviews of Geophysics* **45**: RG2004.

Garreaud RD, Vuille M, Compagnucci R, Marengo J. 2009. Present-day South American climate. *Palaeogeography, Palaeoclimatology, Palaeoecology*. doi: 10.1016/j.palaeo.2007.10.032

Ghiglione MC, Ramos VA. 2005. Progression of deformation and sedimentation in the southernmost Andes. *Tectonophysics* **405**: 25–46.

Gilli A, Anselmetti FS, Ariztegui D, Bradbury JP, Kelts KR, Markgraf V, McKenzie JA. 2001. Tracking abrupt climate change in the Southern Hemisphere: a seismic stratigraphic study of Lago Cardiel, Argentina (49° S). *Terra Nova* **13**: 443–448.

Gilli A, Ariztegui D, Anselmetti FS, Bradbury JP, McKenzie JA, Markgraf V, Hajdas I, McCulloch RD. 2005. Mid-Holocene strengthening of the Southern Westerlies in South America: sedimentological evidences from Lago Cardiel, Argentina (49° S). *Global and Planetary Change* **49**: 75–93.

Girardclos S, Fiore J, Rachoud-Schneider A-M, Baster IRA, Wildi W. 2005. Petit-Lac (western Lake Geneva) environment and climate history from deglaciation to the present: a synthesis. *Boreas* **34**: 417–433.

Haberzettl T, Fey M, Lucke A, Maidana N, Mayr C, Ohlendorf C, Schabitz F, Schleser GH, Wille M, Zolitschka B. 2005. Climatically induced lake level changes during the last two millennia as reflected in sediments of Laguna Potrok Aike, southern Patagonia (Santa Cruz, Argentina). *Journal of Paleolimnology* **33**: 283–302.

Haflidason H, Sejrup HP, Kristensen DK, Johnsen S. 1995. Coupled response of the late glacial climatic shifts of Northwest Europe reflected in Greenland ice cores: evidence from the northern North Sea. *Geology* **23**: 1059–1062.

Heusser CJ. 1989. Late Quaternary vegetation and climate of southern Tierra del Fuego. *Quaternary Research* **31**: 396–406.

Heusser CJ. 1998. Deglacial paleoclimate of the American sector of the Southern Ocean: Late Glacial–Holocene records from the latitude of Canal Beagle (55° S), Argentine Tierra del Fuego. *Palaeogeography, Palaeoclimatology, Palaeoecology* **141**: 277–301.

Hodell DA, Kanfoush SL, Shemesh A, Crosta X, Charles CD, Guilderson TP. 2001. Abrupt cooling of Antarctic surface waters and sea ice expansion in the South Atlantic sector of the Southern Ocean at 5000 cal yr B. P. *Quaternary Research* **56**: 191–198.

Jenny B, Valero-Garcés BL, Villa-Martínez R, Urrutía R, Geyh M, Veit H. 2002. Early to mid-Holocene aridity in central Chile and the Southern Westerlies: the Laguna Aculeo record (34° S). *Quaternary Research* **58**: 160–170.

Kalnay E, Kanamitsu M, Kistler R, Collins W, Deaven D, Gandin L, Iredell M, Saha S, White G, Woollen J, Zhu Y, Chelliah M, Ebisuzaki W, Higgins W, Janowiak J, Mo KC, Ropelewski C, Wang J, Leetmaa A, Reynolds R, Jenne R, Joseph D. 1996. The NCEP/NCAR 40-year reanalysis project. *Bulletin of the American Meteorological Society* **77**: 437–471.

Kilian R, Baeza O, Steinke T, Arevalo M, Rios C, Schneider C. 2007. Late Pleistocene to Holocene marine transgression and thermohaline control on sediment transport in the western Magellanes fjord system of Chile (53° S). *Quaternary International* **161**: 90–107.

Klepeis KA. 1994. The Magallanes and Deseado fault zones: major segments of the South American–Scotia transform plate boundary in southernmost South America, Tierra del Fuego. *Journal of Geophysical Research* **99**: 22001–22014.

Klinger BA, Drijfhout S, Marotzke J, Scott JR. 2003. Sensitivity of basinwide meridional overturning to diapycnal diffusion and remote wind forcing in an idealized Atlantic Southern Ocean geometry. *Journal of Physical Oceanography* **33**: 249–266.

Kutzbach J, Guetter PJ, Behling P, Selin R. 1993. Simulated climatic changes: results of the COHMAP climate-model experiments. In *Global Climates Since the Last Glacial Maximum*, Wright HE, Kutzbach JE, Webb E (eds). University of Minnesota Press: Minneapolis; MN; 24–93.

Kuylenstierna JL, Rosqvist GC, Holmlund P. 1996. Late-Holocene glacier variations in the Cordillera Darwin, Tierra del Fuego, Chile. *The Holocene* **6**: 353–358.

Lamy F, Hebbeln D, Wefer G. 1999. High-resolution marine record of climatic change in mid-latitude Chile during the Last 28,000 years based on terrigenous sediment parameters. *Quaternary Research* **51**: 83–93.

Lamy F, Hebbeln D, Röhl U, Wefer G. 2001. Holocene rainfall variability in southern Chile: a marine record of latitudinal shifts of the Southern Westerlies. *Earth and Planetary Science Letters* **185**: 369–382.

Lamy F, Ruhlemann C, Hebbeln D, Wefer G. 2002. High- and low-latitude climate control on the position of the southern Peru–Chile current during the Holocene. *Paleoceanography* **17**: 16.11–16.10.

Lister GS, Giovanoli F, Eberli G, Finckh P, Finger W, He Q, Heim C, Hsu KJ, Kelts K, Peng C, Sidler C, Zhao X. 1984. Late Quaternary sediments in Lake Zurich, Switzerland. *Environmental Geology* **5**: 191–205.

Ljung K, Bjorck S. 2008. Holocene climate and vegetation dynamics on Nightingale Island, South Atlantic: an apparent interglacial bipolar seesaw in action? *Quaternary Science Reviews* **26**: 3150–3166.

Lodolo E, Menichetti M, Bartole R, Ben-Avraham Z, Tassone A, Lippai H. 2003. Magallanes-Fagnano continental transform fault (Tierra del Fuego, southernmost South America). *Tectonics* **22**: 1076. doi: 10.1029/2003TC001500

Lodolo E, Lippai H, Tassone A, Zanolla C, Menichetti M. 2007. Gravity map of the Isla Grande de Tierra del Fuego, and morphology of Lago Fagnano. *Geologica Acta* **5**: 307–3314.

Mariazzi A, Conzzono V, Ulibarrena J, Paggi J, Donadelli J. 1987. Limnological investigation in Tierra del Fuego, Argentina. *Biología Acuática* **10**: 1–74.

Markgraf V. 1993. Paleoenvironments and paleoclimates in Tierra-Del-Fuego and southernmost Patagonia, South America. *Palaeogeography Palaeoclimatology Palaeoecology* **102**: 53–68.

Markgraf V, Bradbury JP, Schwalb A, Burns SJ, Stern C, Ariztegui D, Gilli A, Anselmetti FS, Stine S, Maidana N. 2003. Holocene palaeoclimates of southern Patagonia: limnological and environmental history of Lago Cardiel, Argentina. *The Holocene* **13**: 581–591.

Mauquoy D, Blaauw M, van Geel B, Borromei A, Quattrochio M, Chambers FM, Possnert G. 2004. Late Holocene climatic changes in Tierra del Fuego based on multiproxy analyses of peat deposits. *Quaternary Research* **61**: 148–158.

McCulloch RD, Bentley MJ, Purves RS, Hulton NRJ, Sugden DE, Clapperton CM. 2000. Climatic inferences from glacial and palaeoecological evidence at the last glacial termination, southern South America. *Journal of Quaternary Science* **15**: 409–417.

Menichetti M, Lodolo E, Tassone A, Geletti R. 2001. Neotectonics at the Magallanes–Fagnano fault system (Tierra del Fuego Island). In *Antarctic Neotectonics Workshop*, Siena; 55.

Menichetti M, Lodolo E, Tassone A. 2008. Structural geology of the Fuegian Andes and Magallanes fold-and-thrust belt: Tierra del Fuego Island. *Geologica Acta* **6**: 19–42.

Moy CM, Dunbar RB, Moreno PI, Francois J-P, Villa-Martínez R, Mucciarone DM, Guilderson TP, Garreaud RD. 2008. Isotopic evidence for hydrologic change related to the westerlies in SW Patagonia, Chile, during the last millennium. *Quaternary Science Reviews* **27**: 1335–1349.

Mullins HT, Hinchey EJ, Wellner RW, Stephens DB, Anderson JWT, Dwyer TR, Hine AC. 1996. Seismic stratigraphy of the Finger Lakes: a continental record of Heinrich event H-1 and Laurentide ice sheet instability. In *Special Paper 311: Subsurface geologic investigations of New York Finger Lakes: implications for late Quaternary deglaciation and environmental change*. Geological Society of America: Boulder, CO; 1–35.

Naranjo JA, Stern CR. 1998. Holocene explosive activity of Hudson Volcano, southern Andes. *Bulletin of Volcanology* **59**: 291–306.

Planas X, Ponsa A, Coronato A, Rabassa J. 2002. Geomorphological evidence of different glacial stages in the Martial cirque, Fuegian Andes, southernmost South America. *Quaternary International* **87**: 19–27.

Porter SC. 2000. Onset of neoglaciation in the Southern Hemisphere. *Journal of Quaternary Science* **15**: 395–408.

Postma D. 1981. Formation of siderite and vivianite and the pore-water composition of a recent bog sediment in Denmark. *Chemical Geology* **31**: 225–244.

Rabassa J, Coronato A, Bujalesky G, Salemme M, Roig C, Meglioli A, Heusser C, Gordillo S, Roig F, Borromei A, Quattrocchio M. 2000. Quaternary of Tierra del Fuego, southernmost South America: an updated review. *Quaternary International* **68**: 217–240.

Rahmstorf S, England MH. 1997. Influence of Southern Hemisphere winds on North Atlantic deep water flow. *Journal of Physical Oceanography* **27**: 2040–2054.

Schnellmann M, Anselmetti FS, Giardini D, McKenzie JA. 2005. Mass movement-induced fold-and-thrust belt structures in unconsolidated sediments in Lake Lucerne (Switzerland). *Sedimentology* **52**: 271–289.

Steig EJ, Brook EJ, White JWC, Sucher CM, Bender ML, Lehman SJ, Morse DL, Waddington ED, Clow GD. 1998. Synchronous climate changes in Antarctica and the North Atlantic. *Science* **282**: 92–95.

Stern CR. 2008. Holocene tephrochronology record of large explosive eruptions in the southernmost Patagonian Andes. *Bulletin of Volcanology* **70**: 435–454.

Tassone A, Lodolo E, Menichetti M, Yagupsky D, Caffau M, Vilas FE. 2008. Seismostratigraphic and structural setting of the Malvinas Basin and its southern margin (Tierra del Fuego Atlantic offshore). *Geologica Acta* **6**: 55–67.

Thompson DWJ, Wallace JM. 2000. Annular modes in the extratropical circulation. Part I: Month-to-month variability. *Journal of Climate* **13**: 1000–1016.

Toggweiler JR, Samuels B. 1995. Effect of Drake Passage on the global thermohaline circulation. *Deep Sea Research Part I: Oceanographic Research Papers* **42**: 477–500.

Unkel I, Björck S, Wohlfarth B. 2008. Deglacial environmental changes on Isla de los Estados (54.4° S), southeastern Tierra del Fuego. *Quaternary Science Reviews* **27**: 1541–1554.

van Rensbergen P, de Batist M, Beck C, Chapron E. 1999. High-resolution seismic stratigraphy of glacial to interglacial fill of a deep glacigenic lake: Lake Le Bourget, Northwestern Alps, France. *Sedimentary Geology* **128**: 99–129.

Waldmann N, Ariztegui D, Anselmetti FS, Austin JJA, Dunbar R, Moy CM, Recasens C. 2008. Seismic stratigraphy of Lago Fagnano sediments (Tierra del Fuego, Argentina): a potential archive of paleoclimatic change and tectonic activity since the Late Glacial. *Geologica Acta* **6**: 101–110.

Wyrwoll K-H, Dong B, Valdes P. 2000. On the position of southern hemisphere westerlies at the Last Glacial Maximum: an outline of AGCM simulation results and evaluation of their implications. *Quaternary Science Reviews* **19**: 881–898.